PCCP

Accepted Manuscript

ROYAL SOCIETY OF CHEMISTRY

www.rsc.org/pccp

A fluorescent receptor for halide recognition: clues for design of anion chemosensors

Riccardo Chelli,[a,b] Giangaetano Pietraperzia,[a,b] Andrea Bencini,[a] Claudia Giorgi,[a] Vito Lippolis,[c] Pier R. Salvi,[a] Cristina Gellini[a,b*]

[a]*Dipartimento di Chimica, Università di Firenze, Via della Lastruccia 3, 50019 Sesto Fiorentino (FI), Italy.*

[b]*European Laboratory for Non-linear Spectroscopy (LENS), Via Nello Carrara 1, 50019 Sesto Fiorentino (FI), Italy.*

[c]*Dipartimento di Scienze Chimiche e Geologiche, Università di Cagliari, S.S. 554 Bivio per Sestu, 09042 Monserrato (CA), Italy.*

Keywords: macrocyclic ligand, fluorescence emission, *ab initio* calculations.

Table of Contents entry:

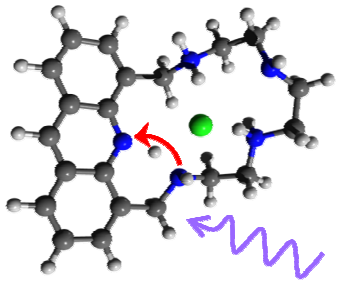

The chemosensing properties of a polyammine ligand containing acridine as chromophore have been investigated by means of emission fluorescence spectroscopy, considering halide ions as substrates. The complex fluorescence emission is due to the acridinium species which are formed after photoinduced proton transfer reaction.

Abstract

The chemosensing properties of the polyaza-macrocycle 1(6,7)-acridine-3,6,9,12-tetraaza-tridecaphane have been investigated by means of emission fluorescence spectroscopy, considering halide ions as substrates. As in the case of the free ligand, the fluorescence emission of the complexes is due to the acridinium species which are formed after photoinduced proton transfer reaction. The complexation constants have been obtained for the bi- and tri-protonated ligands in deoxygenated aqueous solutions. Two different emission behaviours have been observed varying the anion. Fluoride and chloride give rise to fluorescence enhancement whereas bromide and iodide strongly quench the emission. The macrocycle shows an unusual higher selectivity towards the chloride anion rather than fluoride. The fluorescence emission has been modelled considering a modified Stern-Volmer equation, taking into account for the largest anions quenching effects, which can be considered negligible for fluoride and chloride anions. *Ab initio* calculations allow to interpret the fluorescence emission of the complexes in terms of activation energy related to the proton transfer reaction responsible of the emission process.

Introduction

Recognition and sensing of anions have become research areas of increased interest in the field of supramolecular chemistry.[1-8] Anions play a major role in environmental and industrial processes and, more importantly, in biological metabolism where phosphate, carbonate and halide ions are the species most frequently found. In particular, chloride is essential to human health and is transported across cell membranes by various proteins, often in conjunction with cation transportation, while iodide is involved in thyroid physiology.[9,10] On the other hand, fluoride and bromide, though naturally occurring, may be environmental pollutants, both of them being toxic at high concentration levels.[11-14] Fluoride

abatement is a current challenge in water treatment in several world areas.[13,14] Also, bromide is an undesired by-side product of a number of industrial chemical processes.[11] Experimental methods devoted to halide detection in small concentrations and in a real-time and non-destructive mode are actively investigated with the purpose of implementing analytical techniques in biological and environmental studies. Among them, fluorescence chemosensing stands as the spectroscopic tool capable to signal the presence of these anions in real matrices *via* a change of emission properties.[3-8] Usually a fluorescent chemosensor for anion recognition and sensing is structured following the "binding-site signalling subunit" protocol: the binding site is covalently linked to the signalling unit through an appropriate spacer so that the host-guest interaction of the target species with the binding unit modulates the fluorescence of the signalling unit. The binding site is designed to achieve spatial optimization of non-covalent interactions through topological complementarity.[1-8] The task is made difficult in the case of halides in aqueous media as anion solvation by water molecules can strongly compete with binding the receptor unit. At the same time, the spherical shape of halides requires the use of hosts often containing clefts or cavities of appropriate size to lodge the anions.[1-8,15-18]

Polyamines have been often used to bind anions, including halides, in water. In fact, polyamines normally occur as polycharged cations in water solution, even at neutral pH, establishing strong charge-charge and hydrogen bonding interactions with the anionic species, which are a necessary prerequisite for complex coordination in a solvating medium.[1,2] Although several examples of anion binding through encapsulation within cavities or clefts of protonated polyamine macrocycles have been reported,[1-8,19-29] studies on metal-free fluorescent chemosensors in water are mostly selective for the fluoride anion,[30-38] and in any case none of polyammonium type.

Recently, we have reported on the synthesis of the polyaza-macrocycle 1(6,7)-acridine-3,6,9,12-tetraaza-tridecaphane (from now on denoted as **L**; see Fig. 1), which contains a tetraamine chain linked to an acridine unit through ethylene spacers.[39] In principle, while the tetraamine chain, when protonated, constitutes a potential binding site for anions, the fluorescent acridine moiety may act as signalling unit. A preliminary study on the acid-base properties of **L** revealed that the binding and signalling units strongly interact in the lowest excited state and, as a result, a transfer channel opens at intermediate pH values, making possible the migration of an acidic proton from an ammonium group adjacent to the fluorophore to the heteroaromatic nitrogen.[39] An intense fluorescence centered around 450 nm is observed, which was assigned to the acridinium-like fragment of the bi- and tri-protonated species of **L** (from now on indicated with LH_2^{2+} and LH_3^{3+}).[40,41] Its ability in sensing anions relies not only on the stability of the host-guest adduct, but also on the efficiency of the intramolecular proton transfer from the aliphatic polyamine chain to the acridine unit. We can speculate that an appropriate combination of these two factors could selectively enhance the sensing performance for a target anion. To verify this hypothesis, the emission properties of **L** in presence of halide anions have been studied and the results are herein reported.

Experimental

Deoxygenated water solutions of **L**, whose synthesis has been described elsewhere,[39] were carefully prepared as follows. The solution cells, placed inside a glove-box, were bubbled with anhydrous N_2 gas for ≈ 15 minutes and then sealed with rubber caps through which small amounts of anion solution were injected by means of a syringe in absence of air.[a] The glove-box was kept under continuous N_2 flow and equipped with a pH-meter. The anion solutions were prepared by dissolving sodium halides in water with concentration as high as $2 \cdot 10^{-1}$ M and gradually added to the ligand solution, whose concentration C_L is kept constant in a titration experiment ($C_L = 2.5 \cdot 10^{-5}$ M).[43] Then, the fluorescence spectra were measured as a function of the anion concentration, C_S. The total volume variation of the solution during the anion addition was estimated to be less than 5% of the initial 2 cm^3 solution volume. After allowing the solution to reach

equilibrium, fluorescence spectra were measured with a Perkin-Elmer Spectrophotofluorimeter LS-55, set at 10 nm bandwidth for both excitation and emission monochromator slits, exciting at 345 nm in correspondence of the second excited state of **L** and using a 1% neutral density filter for signal attenuation. Before titration, the pH was adjusted to about 5.7, where the concentrations of LH_2^{2+} and LH_3^{3+} are comparable, whereas the species at the other protonation states are negligible.[39] pH adjustement was realized by adding dropwise methanesulfonic acid and sodium hydroxide solutions, and was found to be increased to about 6.7 at the end of titration. Due to difficulties inherent to the experiment, it was not possible to measure the pH after each anion addition. Routine absorption spectra of the same solutions were recorded with a Cary 5 spectrophotometer.

Results

The fluorescence spectra of the ligand complexes with Cl^- and Br^- are reported in Fig. 2. They show a single and very broad unstructured band with maximum at ≈ 450 nm, which is attributed, like in the free ligand case, to the acridinium-like cromophore.[39] It is worth noting that the band intensity increases upon Cl^- addition, whereas it decreases upon Br^- addition. The same opposite trend is observed upon F^-/I^- addition. The comparison with the absorption spectra (not shown), straightforwardly assigned to the acridine cromophore, clearly indicates that the excited state proton transfer, proposed for the free ligand,[39] also occurs in the case of the **L**-halide complexes. The dependence of the fluorescence intensities on C_S, where S = F^-, Cl^-, Br^- and I^-, is shown in Fig. 3. The two points of major interest deal with the total fluorescence intensities:

a) the fluorescence intensity increases adding F^- and Cl^-; the trend is reversed with Br^- and I^- as substrates.

b) a limiting value is observed upon Cl^- and F^- addition at $C_S \approx 5C_{\mathbf{L}}$ and $C_S \approx 12C_{\mathbf{L}}$, respectively. On the contrary, even in the presence of a large excess of Br^- and I^- anions, the fluorescence intensity does not reach a saturation value.

The changes in the fluorescence spectrum according to the anion concentration allow to evaluate the stability constant of the complex. The treatment of 1:1 complexes has been discussed in Ref. 43. This is not however our case, since **L** can bind up to four protons in the pH range 2 – 11 and, as a result, the fluorescence may in principle originate from the free ligand undergoing four protonation steps and the associated complexes. As observed in potentiometric measurements,[39] in the pH range 4.5 – 8.0, the LH_2^{2+} and LH_3^{3+} species are largely dominant and nearly equimolar at pH ≈ 5.7. In these experimental conditions it is therefore reasonable to neglect all the equilibria other than those pertaining to LH_2^{2+} and LH_3^{3+} and their complexes with anions, i.e., SLH_2^+ and SLH_3^{2+}

$$2S^- + LH_2^{2+} + LH_3^{3+} \rightleftharpoons SLH_2^+ + SLH_3^{2+} \qquad K_s = \frac{[SLH_2^+][SLH_3^{2+}]}{[S^-]^2[LH_2^{2+}][LH_3^{3+}]} \qquad (1)$$

$$LH_3^{3+} \rightleftharpoons LH_2^{2+} + H^+ \qquad K_a = \frac{[LH_2^{2+}][H^+]}{[LH_3^{3+}]} \qquad (2)$$

where equilibrium (1) is the result of two separated equilibria:

$$S^- + LH_2^{2+} \rightleftharpoons SLH_2^+ \qquad K_2 = \frac{[SLH_2^+]}{[S^-][LH_2^{2+}]} \qquad (3)$$

$$S^- + LH_3^{3+} \rightleftharpoons SLH_3^{2+} \qquad K_3 = \frac{[SLH_3^{2+}]}{[S^-][LH_3^{3+}]} \qquad (4)$$

with $K_s = K_2K_3$. As already noted, the pH increases whichever the added anion, reaching ≈ 6.7 at the end of the titration. This implies that K_3 is greater than K_2, as only in this case the acid-base equilibrium (2) is shifted toward the tri-protonated species, thus decreasing $[H^+]$. In order to determine K_2 and K_3, the dependence of the fluorescence intensity

on the concentrations of LH_2^{2+}, LH_3^{3+}, SLH_2^{+} and SLH_3^{2+} has been reproduced through a fitting procedure. The model employed in the fit is based on static quenching,[43,44] according to which the fluorescence intensity Y is proportional to the concentrations of the fluorophores and can be thus written as

$$Y = a[LH_2^{2+}] + b[LH_3^{3+}] + c[SLH_2^{+}] + d[SLH_3^{2+}] \quad (5)$$

To fit the measured fluorescence intensities of Fig. 3 using Eq. (5), one needs to determine, in addition to the *a*, *b*, *c* and *d* parameters, the concentrations of the four fluorophores. This can be done employing further equations associated with the chemical equilibria into play. The *a* and *b* parameters have been determined by independent fluorescence measurements on the free ligand as $a = 1.006 \cdot 10^7\ M^{-1}$, $b = 1.070 \cdot 10^7\ M^{-1}$. A detailed description of the fitting procedure is reported in the Appendix. As shown there, the number of fitting parameters can be limited to three, namely *c* and *d* and K_s. Once K_s is known, K_2 and K_3 can be evaluated by solving chemical equations at a given arbitrary C_S and using the calculated concentrations into Eqs. (3) and (4). The values of the fitting parameters together with χ^2, the quality index for fitting (see Appendix for definition), and the K_2 and K_3 constants of the SLH_2^{+} and the SLH_3^{2+} complexes are reported in Table I. For the F^- and Cl^- complexes the *c* and *d* parameters are sufficiently accurate, as it is evident looking at the percent errors (less than 4%) and at χ^2. As a result, the calculated profiles of Fig. 4 fit the experimental points remarkably well. The large K_s indicates that both equilibria are strongly shifted toward complexation upon anion addition. Furthermore, K_3 is one order of magnitude greater than K_2, indicating that the tri-protonated complexes are more stable than the bi-protonated ones. Finally, Cl^- results a better target anion than fluoride, being the corresponding K_s more than one order of magnitude greater than that of F^-. On the contrary, the large χ^2 values relative to Br^- and I^- point to the fact that Eq. (5) is unable to reproduce the fluorescence dependence on C_S for these anions (see also Fig. 4). As a matter of fact, their *c* and *d* parameters are affected by large errors so that it is arguable to trust the derived K_2 and K_3 constants.

To improve the agreement with experimental data in the case of Br^- and I^- anions, it should be realized that the static quenching model neglects fluorescence deactivation processes of growing importance when large quantities (100 equivalents or more) of strong fluorescence quenchers, such as Br^- and I^-, are added to the solution. The idea is that additional mechanisms are switched on, which may contribute to the fluorescence decrease much more than what is accounted by Eq. (5). The first one is the so-called collisional or dynamical quenching, generally described by the Stern-Volmer equation,[43,44] which is based on a mechanism involving collisions between excited fluorophore and quencher. Moreover, with abundant quencher concentration, a second deactivation channel may open, which has been related to the sphere of action surrounding the fluorophore within which the probability of immediate quenching is unity.[44] Briefly, if a fluorophore is excited when a quencher is inside the sphere of action, the fluorophore becomes dark. Considering the high anion concentration reached during titration, the above additional quenching mechanism could be relevant for the bi- and tri-protonated free ligands and their Br^- and I^- complexes. For this reason, it is convenient to move from Eq. (5) to the modified Stern-Volmer equation that can be recovered straightforwardly following the guidelines of Ref. 44:

$$Y = \frac{e^{-\alpha[S^-]}}{1+\beta[S^-]}\{a[LH_2^{2+}] + b[LH_3^{3+}] + c[SLH_2^{+}] + d[SLH_3^{2+}]\} \quad (6)$$

where the collisional and proximity quenching contributions are represented by the denominator and the exponential term, respectively, both depending on $[S^-]$. The parameters α and β have been treated on the same basis as *c* and *d* in the fitting procedure, as explained in the Appendix. In principle, α and β depend on the specific fluorophore; however,

a reasonable simplification would be to assume unique values for all the four species, LH_2^{2+}, LH_3^{3+}, SLH_2^{+} and SLH_3^{2+}. For the F^- and Cl^- complexes, adopting Eq. (6) does not alter substantially the results of the static quenching model (see Fig. 4a, 4b and Fig. 5a, 5b), probably because the collisional and proximity quenching mechanisms become important only at higher anion concentrations. As a consequence, a large degree of indetermination on α and β is obtained, and thus for these anions we will keep the outcomes of the static quenching model. On the contrary, it is found that these contributions are essential to obtain a good match between experimental and fitted data for the Br^- and I^- complexes, as we can infer comparing Fig. 4c, 4d and Fig. 5c, 5d. The fitting parameters for these complexes are reported in Table II. Due to the increased extension of the sphere of action and stronger spin-orbit coupling of I^- with respect to Br^-, α and β are higher in the same order. The K_2 constants of the Br^- and I^- complexes are three orders of magnitude smaller than K_3; thus to a very good approximation, only the tri-protonated ligand is responsible of the complexation with Br^- and I^-. This is the reason why the *c* parameters reported in Table II results to be undetermined. In conclusion, Tables I and II show that the F^- and Cl^- complexes have stability constants K_s at least six orders of magnitude larger than those of the Br^- and I^- complexes. This fact and the occurrence of the collisional and proximity quenching processes explain fairly good the absence of a saturation value for the latter pair.

Discussion

As reported in the previous Section, the dependence of the fluorescence intensities on halide addition differs considerably for the two pairs, F^-/Cl^- on one side and Br^-/I^- on the other. The property is discussed here in relation to the intramolecular proton transfer, which is responsible of the fluorescence behaviour of the free ligand as a function of pH.[39,45] The process is assumed to occur in the excited state and to consist of the proton migration from the so-called "chain-protonated" isomer (A) to the "acridine-protonated" isomer (B) (see Fig. 6 for a sketch of the structures). The related activation energy can be calculated by searching for the transition state between the minimum energy structures of the A and B isomers. Two transition states, relative either to the S_1 or to the S_2 electronic states, should be considered for the A* → B* migration process, where the asterisks indicate that the process occurs in an excited state. Starting from the A and B minimum energy structures of the protonated ligands,[39] we have found the stable A and B geometries for all the bi- and tri-protonated anion complexes checking for the absence of normal modes with imaginary frequencies. All calculations were carried out with the Gaussian09 program[46] within the polarizable continuum model for water,[47] by using DFT and time-dependent DFT for ground and excited states, respectively, supplied with the B3-LYP exchange-correlation functional and the 6-31++G(d,p) basis set. Only results on F^-, Cl^- and Br^- are reported, since the employed basis set is not implemented for I^-. The atomic Cartesian coordinates of the optimized geometries of the A and B isomers and of the relative transition states are reported in the Supplementary Information (for the tri-protonated complexes, graphical views of the structures are also reported). The transition state between the A and B isomers is located through the Synchronous Transit-Guided Quasi-Newton method[48] as implemented in the Gaussian09 program. Authentic transition states, i.e. saddle points on the ground state energy surface, are recognized by the occurrence in the vibrational calculation of only one normal mode with imaginary frequency, that approximately corresponds to the H^+ motion along the line connecting the ammonium and the acridine nitrogen atoms. A schematic representation of our procedure is given in Fig. 6, where the A → B path for the tri-protonated F^- complex is displayed. The S_0 energy level of the B isomer lies 8.9 kcal/mol above that of A isomer and the A → B activation energy amounts to 17.2 kcal/mol. Transition states in the ground state of the tri-protonated free ligand and of its Cl^- and Br^- complexes have activation energies of 10.6, 13.3 and 13.6 kcal/mol, respectively (see Table III). Since the tri-protonated free ligand has the lowest activation energy,

assuming these values to hold also for the A* → B* process, a decrease of the fluorescence intensity would be expected for all complexes with respect to the free ligand, in apparent contrast with experiment. Although energy barrier heights in the excited state are more difficult to evaluate, their knowledge is required and here an attempt to the calculation is made considering the vertical excitation energies. First, the $S_0 \rightarrow S_1$ and $S_0 \rightarrow S_2$ energies are calculated by means of the time-dependent DFT in the singly-excited configuration interaction scheme for a total of excited configurations ranging between $\approx 3.9 \cdot 10^4$ (free ligand) and $\approx 4.2 \cdot 10^4$ (Br^- complex) and promoting electrons from all occupied valence orbitals to the whole set of virtual orbitals. To be more specific, these energies refer to the $\pi\pi^*$ transitions of the aromatic chromophore, acridine and acridinium-like ion. In the F^- case, $S_0 \rightarrow S_1$ excitation energies are found at 74.2, 70.0, 59.8 kcal/mol from the minima of the A and B isomers and from the saddle point of the transition state, respectively. The corresponding $S_0 \rightarrow S_2$ data are 84.8, 72.0, 68.8 kcal/mol. For the sake of clarity, these results are reported in Fig. 6. Combining the excitation energies with the ground state calculation, the S_1/S_2 barrier heights are proposed to be the difference between the vertical energies of the transition state and of A*, equal to 13.0 and 4.4 kcal/mol for the S_1 and S_2 states, respectively, of the F^- complex. This assumption can be justified on the basis of the following argument. In a previous *ab initio* study,[49] the two lowest $\pi\pi^*$ states of acridine were described mostly in terms of HOMO, LUMO, HOMO−1 and LUMO+1 orbitals, the $S_1(2A_1)$ state involving the singly-excited HOMO → LUMO configuration and the $S_2(1B_2)$ state the symmetric combination of the HOMO−1 → LUMO and HOMO → LUMO+1 configurations. It was further noted the close similarity between these states and the lowest $\pi\pi^*$ states of the acridinium ion.[49] We have replicated the calculation for acridine and for the acridinium ion and extended to the bi- and tri-protonated free ligand, to the respective halide complexes (in the A and B forms) and to the transition states, thus establishing the correlation between the lowest excited states of our systems and those of the isolated cromophores. The true activation energy in the excited state is the difference between the excited state saddle point and the A* minimum, which may be calculated if the relaxation energies from vertical excitations, the first to the excited saddle point and the second to the A* minimum, are known. It is our assumption that the relaxation energies, though in principle different, are substantially similar each to the other. As a test of our hypothesis, the S_1 and S_2 minima of acridine/acridinium ion have been located, and the relaxation energies have been found to be 6.9/5.8 kcal/mol for S_1 and 4.4/2.8 kcal/mol for S_2, i.e., values which are for each pair considerably close. Extrapolating to ligands and complexes, the relaxation energies of the transition states are expected to be equal to those of A within at most 1.1 kcal/mol for S_1 and 1.6 kcal/mol for S_2. The results of Fig. 6 are estimates along this line of reasoning for the F^- complexes in the S_1 and S_2 states. All the activation energies of the other complexes and of the bi- and tri-protonated free ligand have been calculated and reported in Table III. It should be noted from the Table that i) the activation energies of the complexes are greater than that of the protonated ligands except for S_2 of LH_3^{3+} and ii) among these, the lowest value is found for the Cl^- complex.

In principle, the overall process starting from the A excitation and terminating with the B fluorescence can be described by a two-way scheme, where the proton transfer can be accomplished in the S_2 and/or in the S_1 excited state. Since the reduction of the activation energy is a necessary condition to observe fluorescence increase upon anion addition, it is plausible to hypothesize that after excitation in S_2, the F^- and Cl^- tri-protonated complexes undergo proton transfer preferentially in this state, where their energy barriers are lower than that of the free tri-protonated ligand. The same argument would predict a fluorescence increase also upon Br^- addition. In this case, however, it should be further considered that the stability constant K_s of the tri-protonated Br^- complex is at least six orders of magnitude lower than those of the F^- and Cl^- complexes (see Table II). Therefore, at low anion concentrations, where only static quenching mechanism related to spin-orbit coupling in the complex is relevant, the contribution to fluorescence of the few Br^-

complexes is negligible, while at higher concentration the dynamical and proximity quenching dominate. Thus, for both concentration regimes the activation energy plays a minor role in determining the fluorescence dependence on concentration. The same considerations reasonably apply also to the I^- case.

Finally, it is of interest to note that according to the present data both bi- and tri-protonated species of **L** exhibit selectivity for chloride over fluoride. This result appears somewhat unusual, since most synthetic receptors show an opposite behavior, e.g., selectivity for fluoride over chloride.[30-38] Selective binding of fluoride is generally attributed to the ability of the smaller F^- anion to form stronger hydrogen bonds, with a consequent enthalpic stabilization of the complex, and/or to the higher solvation of this anion, which can leads to a marked entropic gain upon complexation.[1,2] However, other factors can contribute to the stabilization of the complexes with anionic species. For instance, comparing the structures of the tri-protonated F^- and Cl^- complexes with **L**, which are shown in Fig. 7, F^- appears almost encapsulated within the macrocycle framework, while Cl^- is located above the macrocycle cavity. The binding mode of fluoride leads to the formation of stronger hydrogen bonding interactions, but also to a marked stiffening of the receptor structure, which may result in an overall lower thermodynamic stability of the complex with respect to that with chloride. These structural observations can also be used to attempt an explanation of the more marked enhancement of fluorescence emission of the receptor upon chloride binding. The proton transfer process can be kinetically less favored by the formation of strong hydrogen bonding interactions between the anion and the ammonium groups of the receptor, as actually observed in the case of the fluoride complex. Therefore, a higher activation energy of the excited state proton transfer process is expected for the fluoride complex with respect to chloride (see Table III).

Examples of fluorogenic receptors able to selectively sense chloride, and overall fluoride in pure water or in water containing mixtures are known.[1-8, 30-38] The use of mixed solvents and/or the formation of complexes with anion-receptor stoichiometry different from 1:1, strongly limit the possibility to make a reliable comparison with the stability of our complexes. However, a pyreneboronic acid-based chemosensor for fluoride in water with an unprecedented high binding constant for fluoride has been recently reported.[38] The constant for the formation of the 1:1 complex was evaluated higher than 10^3, that is lower than those found for the protonated species of **L**. This confirms that polyammonium macrocycles undoubtedly represent a promising challenge to develop receptors able to strongly bind and sense fluoride in water.

Conclusions

The fluorescence properties of halide complexes of **L** have been studied as a function of halide concentrations in the pH region around 6 where the bi- and tri-protonated ligands are the most abundant species. As for the free ligand, the anion complex emission has been ascribed to the acridinium moiety that is formed following an intramolecular proton transfer in the excited states. Two different behaviours have been observed upon anion addition, i.e., fluorescent increment for the F^-/Cl^- pair and quenching for the Br^-/I^- pair. The fluorescence data have been discussed on the basis of a static quenching model implemented by considering dynamical and proximity effects for the heavier Br^-/I^- pair. The model has allowed to estimate the stability constants of the bi- and tri-protonated complexes resorting to a fitting procedure of the fluorescence data. Fluoride and chloride form the more stable complexes; in all four cases the bi-protonated complexes are weaker than the corresponding tri-protonated. The increasing fluorescence emission upon F^- and Cl^- addition has been explained considering how the population of the fluorescent state is affected by the presence of anions. The excitation of the complex in the S_2 state activates a proton transfer process whose energy barrier is varied by the anion complexation. The reduction of the activation energy is the driving condition for observing the fluorescence increase. *Ab initio* calculations of activation energies have been performed and the results show that such a lowering is

obtained in the S_2 state of the tri-protonated forms. The most pronounced effect is predicted for the Cl^- anion. At variance, the fluorescence of the Br^-/I^- complexes is dominated by the dynamical and proximity quenching mechanisms. The anion selectivity decreases in the order Cl^-, F^-, Br^-/I^-.

In conclusion, the ability of **L** in sensing anions depends not only on the stability of the complex itself, but also on the kinetic barrier for the intramolecular proton transfer from the protonated polyamine chain to the acridine unit. From this point of view, encapsulation of the anion within the receptor cavity, as observed in the case of fluoride, induces the formation of strong anion-NH_2^+ hydrogen bonds, which can partially inhibit the proton transfer to the acridine nitrogen.

Supplementary Information

Graphical views of the tri-protonated complex structures.

Atomic Cartesian coordinates of the optimized geometries of both A and B isomers and relative transition states of bi- and tri-protonated F^-, Cl^- and Br^- complexes.

References

1 K. Bowman-James, A. Bianchi and E. García-España, Anion Coordination Chemistry 2012; Wiley-VCH, New York.

2 J.L. Sessler, P.A. Gale and W.S. Cho, Anion Receptor Chemistry 2006; The Royal Society of Chemistry, Cambridge, UK.

3 V. Amendola and L. Fabbrizzi, *Chem. Commun.*, 2009, 513.

4 R. Martínez-Máñez and F. Sancenón, *Chem Rev.*, 2003, **40**, 4419.

5 M.E. Moragues, R. Martínez-Máñez and F. Sancenón, *Chem. Soc. Rev.*, 2011, **40**, 2593.

6 L.E. Santos-Figueroa, M.E. Moragues, E. Climent, A. Agostini, R. Martínez-Máñez and F. Sancenón, *Chem. Soc. Rev.*, 2013, **42**, 3489.

7 M. Wenzel, J.R. Hiacok and P.A. Gale, *Chem. Soc. Rev.*, 2012, **41**, 480.

8 C. Caltagirone and P.A. Gale, *Chem. Soc. Rev.*, 2009, **38**, 520.

9 A.P. Davis, D.N. Sheppard and B.D. Smith, *Chem. Soc. Rev.*, 2007, **36**, 348.

10 D. L. Nelson and M. M. Cox, Lehninger Principles of Biochemistry, 5th edn, W. H. Freeman, NY, 2009.

11 M. Flury and A. Papritz, *J. Environ. Qual.*, 1993, **22**, 747.

12 A. Vengosh and I. Pankratov, *Groundwater*, 1998, **36**, 815.

13 S. Peckham and N. Awofeso, *Sci. World J.*, 2014, 1.

14 S. Ayoob and A.K. Gupta, *Critical Review in Environmental Science and Technology*, 2006, **36**, 433.

15 A.P. Davis and J.B. Joos, *Coord. Chem. Rev.*, 2003, **240**, 143.

16 J.M. Boon and B.D. Smith, *Curr. Opin. Chem. Biol.*, 2002, **6**, 749.

17 B.A. McNally, A.V. Koulov, B.D. Smith, J.B. Joos and A.P. Davis, *Chem. Commun.*, 2005, 1087.

18 P. D. Beer and P. A. Gale, *Angew. Chem., Int. Ed. Eng.*, 2001, **40**, 486.

19 L. Fabbrizzi, M. Licchelli, G. Rabaioli and A. Taglietti, *Coord. Chem. Rev.* 2000, **205**, 59.

20 J. M. Llinares, D. Powell and K. Bowman-James, *Coord. Chem. Rev.*, 2003, **240**, 57.

21 V. McKee, J. Nelson and R. M. Town, *Chem. Soc. Rev.*, 2003, **32**, 309.

22 C. Miranda, F. Escarti, L. Lamarque, M. J. R. Yunta, P. Navarro, E. Garcia-España and M. L. Jimeno, *J. Am. Chem. Soc.*, 2004, **126**, 823.

23 B. P. Hay, M. Gutowski, D. A. Dixon, J. Garza, R. Vargas and B. A. Moyer, *J. Am. Chem. Soc.*, 2004, **126**, 7925.

24 C. A. Ilioudis, D. A. Tocher and J. W. Steed, *J. Am. Chem. Soc.*, 2004, **126**, 12395.

25 P. A. Gale, *Coord. Chem. Rev.*, 2003, **240**, 191.

26 J. L. Sessler, S. Camiolo and P. A. Gale, *Coord. Chem. Rev.*, 2003, **240**, 17.

27 C. Anda, A. Llobet, A. E. Martell, J. Reibenspies, E. Berni and X. Solans, *Inorg. Chem.*, 2004, **43**, 2793.

28 S. D. Reilly, G. R. K. Khalsa, D. K. Ford, J. R. Brainard, B. P. Hay and P. H. Smith, *Inorg. Chem.*, 1995, **34**, 569.

29 B. Dietrich, B. Dilworth, J.-M Lehn, J.-P. Souchez, M. Cesario, J. Guilhem and C. Pascard, *Helv. Chim. Acta*, 1996, **79**, 569.

30 L. Trembleau, T. A. D. Smith and M. H. Abdelrahman, *Chem. Commun.*, 2013, **49**, 5850.

31 M. Hirai and F.P. Gabbai, *Chemical Science*, 2014, **5**, 1886.

32 A.K. Mahapatra, R. Maji, K. Maiti, S.S. Adhikari, C. Das Mukhopadhyay and D. Mandal, *Analyst*, 2014, **139**, 309.

33 K. Kanagaraj and K. Pitchumani, *Chemistry - Asian J.*, 2014, **9**, 146.

34 T. Nishimura, S.-Y. Xu, Y.-B. Jiang, J.S. Fossey, K. Sakurai, S.D. Bull and T.D. James, *Chem. Commun.*, 2013, **49**, 478.

35 R. Hu, J. Feng, D. Hu, S. Wang, S. Li, Y. Li and G. Yang, *Angew. Chem.*, 2010, **49**, 4915.

36 S.Y. Kim, J. Park, M. Koh, S.B. Park and J.-In Hong, *Chem. Commun.*, 2009, 4735.

37 Y. Kubo, T. Ishida, A. Kobayashi and T.D. James, *J. Materials Chem.*, 2005, **15**, 2889.

38 X. Wu, X.-X. Chen, B.-N. Song, Y.-J. Huang, W.-J. Ouyang, Z. Li, T. D. James and Y.-B. Jiang, *Chem. Commun.*, 2014, 13987.

39 S. Puccioni, C. Bazzicalupi, A. Bencini, C. Giorgi, B. Valtancoli, G. De Filippo, V. Lippolis, P.R. Salvi, G. Pietraperzia, R. Chelli and C. Gellini, *J. Phys. Chem. A*, 2013, **117**, 3798.

40 M.K. Sarangi, D. Dey and S. Basu, *J. Phys. Chem. A*, 2011, **115**, 128.

41 M.K. Sarangi and S. Basu, *Phys. Chem. Chem. Phys.*, 2011, **13**, 16821.

42 J.B. Birks, Photophysics of Aromatic Molecules, Wiley – Interscience, London, 1970.

43 B. Valeur, Molecular Fluorescence. Principle and Applications. Wiley-VCH, Weinheim, 2002.

44 J. R. Lakowicz, Principles of Fluorescence Spectroscopy, 3rd Edition, Springer 2006 and reference therein.

45 C.A. Smith, H.-C. Chang, W.S. Struve, G.J. Atwell and W.A. Denny, *J. Phys. Chem.*, 1995, **99**, 8927.

46 M.J. Frisch, G.W. Trucks, H.B. Schlegel, G.E. Scuseria, M.A. Robb, J.R. Cheeseman, G. Scalmani, V. Barone, B. Mennucci, G.A. Petersson et al. Gaussian 09, Revision A.1; Gaussian, Inc.: Wallingford, CT, 2009.

47 J. Tomasi, B. Mennucci and R. Cammi, *Chem. Rev.*, 2005, **105**, 2999.

48 C. Peng and H.B. Schlegel, *Israel J. Chem.*, 1993, **33**, 449.

49 O. Rubio-Pons, L. Serrano-Andres and M. Merchan, *J. Phys. Chem. A*, 2001, **105**, 9664.

50 R. Chelli, V.V. Volkov and R. Righini, *J. Comput. Chem.*, 2008, **29**, 1507.

[a] Due to oxygen quenching the same experiments with aerated solutions showed small variations of the fluorescence spectrum, if any, upon addition of substrate. This may be reasonably ascribed to the fluorescence lifetime of the acridinium cromophore, larger than the diffusion-controlled oxygen-quenching time constant, ≈ 20 ns.[42]

Tables

Table I. Fitting parameters *c*, *d* and $\log K_s$, obtained by using Eq. (5) for the F^-, Cl^-, Br^- and I^- complexes (see Fig. 4 for graphical outcomes). Derived stability constants, $\log K_2$ and $\log K_3$, are also given. The uncertainties are estimated as described in the Appendix.
[a] The value in parenthesis represents an upper limit for that parameter.
[b] "und" stands for "undetermined" (see Appendix).

	F^-	Cl^-	Br^-	I^-
$\log K_s$	9.6 ± 0.2	11.2 ± 0.3	4.9 ± 0.5	5.0 ± 0.8
$\log K_2$	4.1 ± 0.1	5.0 ± 0.2	1.9 ± 0.5	1.8 (< 2.1)[a]
$\log K_3$	5.5 ± 0.1	6.2 ± 0.1	3.0 ± 0.2	3.2 ± 0.3
$c / 10^7$ (M^{-1})	2.51 ± 0.09	1.42 ± 0.06	und[b]	und[b]
$d / 10^7$ (M^{-1})	1.14 ± 0.03	1.46 ± 0.02	0.16 ± 17	0.06 ± 21
χ^2	19.0	8.6	420	863

Table II. Fitting parameters *c*, *d* and $\log K_s$, obtained by using Eq. (6) for the Br^- and I^- complexes (see Fig. 5c and 5d for graphical outcomes). Derived stability constants, $\log K_2$ and $\log K_3$, are also given. The uncertainties are estimated as described in the Appendix.
[a] The value in parenthesis represents an upper limit for that parameter.
[b] "und" stands for "undetermined" (see Appendix).

	Br^-	I^-
$\log K_s$	2.6 (< 3.8)[a]	2.9 (< 3.7)[a]
$\log K_2$	–0.2 (< 0.98)[a]	-0.06 (< 0.7)[a]
$\log K_3$	2.78 ± 0.01	2.96 ± 0.02
c (M^{-1})	und[b]	und[b]
$d / 10^7$ (M^{-1})	1.39 ± 0.02	2.50 ± 0.04
β (M^{-1})	214 ± 5	609 ± 12
α (M^{-1})	29 ± 3	41 ± 5
χ^2	0.83	1.37

Table III. Transition state activation energies (kcal/mol) of the excited state proton transfer process calculated for the bi- and tri-protonated forms of the free ligand and their complexes with halides.

LH_3^{3+}	L	LF	LCl	LBr
S_0	10.6	17.2	13.3	13.6
S_1	7.1	13.0	9.6	8.7
S_2	10.1	4.4	1.7	3.0
LH_2^{2+}				
S_0	7.9	17.1	12.5	12.9
S_1	2.0	4.4	1.3	2.7
S_2	-1.2	9.2	4.9	2.3

Captions to the Figures

Figure 1 – Structural formula of 1-(6,7)-acridine-3,6,9,12-tetraaza-tridecaphane (**L**).

Figure 2 – Fluorescence emission spectra of **L** complexes with Cl^- (upper panel) and Br^- (lower panel) as a function of added anion equivalents. Same colours in the two panels refer to the same order of anion addition. The arrows indicate that the fluorescence intensity increases/decreases upon chloride/bromide addition.

Figure 3 – Fluorescence intensity dependence on the anion concentration measured for the **L** complexes with F^-, open circles, and Cl^-, stars, (upper panel) and Br^-, open circles, and I^-, stars, (lower panel). Intensities are normalized with respect to those of the free ligand.

Figure 4 – Fitting curves calculated by using Eq. (5). Fluoride complex (panel a), chloride complex (panel b), bromide complex (panel c), iodide complex (panel d). Intensities Y are normalized with respect to those of the free ligand Y_0.

Figure 5 – Fitting curves calculated by using the Eq. (6). Fluoride complex (panel a), chloride complex (panel b), bromide complex (panel c), iodide complex (panel d). Intensities Y are normalized with respect to those of the free ligand Y_0.

Figure 6 – A → B reaction path for the tri-protonated F^- complex. Black line S_0, blue line S_1, red line S_2. Dashed arrows represent activation energies (see Table III) expressed in kcal/mol. Solid arrows represent $S_0 \rightarrow S_2$ excitation and $S_1 \rightarrow S_0$ fluorescence emission as in the experiment. At the bottom a simplified scheme of A and B structures is sketched. Coloured lines are guides for eyes.

Figure 7 – Calculated ground state structures of the tri-protonated A-type **L** complexes with F^- (panel a) and Cl^- (panel b); left: top view, right: side view. Hydrogen bond distances (Å) between anions and adjacent H atoms are shown.

Appendix

For a diluted solution of a fluorophore in the so-called static quenching regime, i.e., assuming that collisional contributions to quenching are negligible, the fluorescence intensity, Y, can be shown to be proportional to the concentration of the fluorophore.[43,44] In the presence of several fluorophores, the fluorescence intensity of the solution can be approximated as the sum of single fluorophore contributions. In our case, Eq. (5), that we report here for the sake of convenience, can be used

$$Y = a\left[LH_2^{2+}\right] + b\left[LH_3^{3+}\right] + c\left[SLH_2^{+}\right] + d\left[SLH_3^{2+}\right] \qquad (A1)$$

As stated in the Results section, upon considering the working pH range of 5.7 – 6.7, the contributions to Y of the species with protonation states different from 2 and 3 can be neglected and therefore they do not appear into Eq. (A1). In spite of this strong simplification of the problem, the system still remains rather complicated, as four different fluorophores are, in principle, simultaneously present in solution. In order to further simplify the treatment, we have recovered the *a* and *b* parameters resorting to independent fluorescence measurements as follows. Let Y_0 be the fluorescence intensity of the solution containing only analytic concentrations $C_{\mathbf{L}}$, C_{NaOH} and C_A of ligand, sodium hydroxide and methanesulfonic acid, respectively. Then, according to Eq. (A1), Y_0 can be expressed as

$$Y_0 = a\left[LH_2^{2+}\right]_0 + b\left[LH_3^{3+}\right]_0 \qquad (A2)$$

where the subscript 0 indicates the concentrations without anion additions. Once $C_{\mathbf{L}}$, C_{NaOH} and C_A are known along with the equilibrium constant K_a (Eq. (2)), determining LH_2^{2+} and LH_3^{3+} is straightforward. Such an information together with the experimental measure of Y_0, allows to establish a relation between *a* and *b*, via Eq. A2. Moreover, the ratio *a/b* can be obtained from two independent measurements of the fluorescence intensities of the species LH_2^{2+} and LH_3^{3+}, say $Y_0(LH_2^{2+})$ and $Y_0(LH_3^{3+})$. Such measurements have been realized at the same ligand concentration $C_L = 2.5 \cdot 10^{-5}$ M, while tuning the pH at a value for which the concentration of one species is, in turn, maximum and, simultaneously, the concentrations of the other species are negligible (see the potentiometric measurements in Ref. 38). The maximum concentrations of LH_3^{3+} and LH_2^{2+} occur at pH 4.5 and 8, respectively. Thus, exploiting Eq. (A1), we obtain the relations $Y_0(LH_2^{2+}) \approx a\, C_{\mathbf{L}}$ and $Y_0(LH_3^{3+}) \approx b\, C_{\mathbf{L}}$, which allow to find the ratio as

$$a/b \approx Y_0(LH_2^{2+}) / Y_0(LH_3^{3+}) \approx 0.94 \qquad (A3)$$

From Eqs. (A2) and (A3), we can therefore calculate the values of both *a* and *b*, that will be taken as fixed parameters during the fit: $a \approx 1.006 \cdot 10^7\ M^{-1}$, $b \approx 1.070 \cdot 10^7\ M^{-1}$.

Upon fixing *a* and *b*, the remaining unknowns in Eq. (A1) are *c*, *d*, $[LH_2^{2+}]$, $[LH_3^{3+}]$, $[SLH_2^{+}]$ and $[SLH_3^{2+}]$. While *c* and *d* are taken as fitting parameters, the concentrations are determined by solving a system of five (chemical) equations, namely Eqs. 1 and 2 and the following ones:

$$C_S = [S^-] + [SLH_2^{+}] + \left[SLH_3^{2+}\right] \qquad (A4)$$

$$C_{\mathbf{L}} = \left[LH_2^{2+}\right] + \left[LH_3^{3+}\right] + [SLH_2^{+}] + \left[SLH_3^{2+}\right] \qquad (A5)$$

$$2\left[LH_2^{2+}\right] + 3\left[LH_3^{3+}\right] + [SLH_2^{+}] + 2\left[SLH_3^{2+}\right] + [H^+] + [Na^+] = [S^-] + [OH^-] + [CH_3SO_3^-] \qquad (A6)$$

In Eq. (A6), $[Na^+]$ corresponds to the sum of the analytic concentrations of sodium halide (namely C_S), and sodium hydroxide, $[CH_3SO_3^-]$ to the analytic concentration of methanesulfonic acid (the last two, used to tune the initial pH) and $[OH^-] = K_w/[H^+]$. Note that, as in Eq. (1) the constant K_s is unknown, we take it as a fitting parameter. This leads to five equations with six unknown variables: $[LH_2^{2+}]$, $[LH_3^{3+}]$, $[SLH_2^{+}]$, $[SLH_3^{2+}]$, $[S^-]$ and $[H^+]$. Assuming the pH values as further fitting parameters would be unfeasible, because it would lead to many additional parameters, one for each C_S at which Y has been measured. The fit would clearly be ill-conditioned. To tackle this difficulty, we have adopted the self-consistent procedure detailed below.

1) The $[H^+]$ dependence on C_S is first guessed as linear between the initial and final values of C_S, both pH being experimentally known.
2) Once the pH is established for all C_S as stated at point (1), we can solve the system of Eqs. 1, 2, A4, A5 and A6 for each C_S, to eventually find the concentrations of the four fluorophores needed into Eq. (A1) to compute Y as a function of C_S. This allows to carry on the fit of the experimental Y curve obtaining a first-iteration set of values for the fitting parameters *c*, *d* and K_s. The minimized target function is $\chi^2=\left[\sum_{i=1}^{n}\left(Y_{calc,i}^2\text{-}Y_{exp,i}^2\right)\right]1/n$, where *n* is the number of different C_S concentrations used in the titration. It should be noted that, for the value of K_s obtained in the fit, the concentrations $[LH_2^{2+}]$, $[LH_3^{3+}]$, $[SLH_2^{+}]$, $[SLH_3^{2+}]$, and $[S^-]$ may give K_2 and K_3 constants (via Eqs. 3 and 4) that differ each other under different C_S. This unphysical outcome is a consequence of having enforced an arbitrary dependence of pH vs. C_S (see point (1)).
3) Since the pH value at the final C_S of the titration is not guessed but experimentally determined, the corresponding values of K_2 and K_3 will be pH-consistent. Therefore, by using these values of K_2 and K_3, a new set of pH values can be found (one for each concentration C_S) by solving the system of Eqs. 2, 3, 4, A4, A5 and A6 with respect to the variables $[LH_2^{2+}]$, $[LH_3^{3+}]$, $[SLH_2^{+}]$, $[SLH_3^{2+}]$, $[S^-]$ and just $[H^+]$. Note that, as K_2 and K_3 are the same for all C_S, the resulting pH values will be in general different from those established at the point (1) of this procedure, apart from the final pH, which will remain unchanged owing to the pH consistency of K_2 and K_3. Of course, also the initial pH will be unchanged, as in this case the solution is anion free.
4) Using the new set of pH values, steps (2) and (3) are repeated until self-consistency is reached and the pH variations become negligible for all C_S, upon subsequent iterations.

Uncertainty on a fitting parameter is estimated by increasing and decreasing, in turn, the parameter until the χ^2 doubles with respect to its minimum value (fit outcome), keeping fixed all the other fitting parameters. The error is taken to be the absolute value of the largest variation in the fitting parameter.[50] For some fitting parameters, variations in one or both directions (increase/decrease) may result in no appreciable changes of χ^2. This occurs when variations of the parameter as large as ~100% the value obtained from the fit are not sufficient to double χ^2. In the former case (no χ^2 changes upon variation of the fitting parameter in only one direction), we can provide the error as an upper or lower limit of the parameter (actually, we only observed upper limits, as decreasing the parameter does not lead to appreciable χ^2 changes); this is the case, for example, of the $\log K_s$ parameter in Table II. In the latter case (no χ^2 changes upon variation of the fitting parameter in both directions), the parameter is classified as undetermined; see, for example, the *c* parameter of Br^- and I^- in Table I.

The errors on the derived quantities, $\log K_2$ and $\log K_3$, correspond to their largest change when increase and decrease of $\log K_s$ doubles χ^2. In the case of Table II, it could appear anomalous that, while only upper limits are provided for $\log K_s$ and $\log K_2$, a quite precise evaluation is reported for $\log K_3$. This is due to the small variation of $\log K_3$, relatively to its absolute value, when varying $\log K_s$. As an example, we discuss the case of I^- (Table II). The fitting outcomes for $\log K_s$, $\log K_2$ and $\log K_3$ are 2.9, −0.06 and 2.96, respectively, with χ^2=1.37. Increasing $\log K_s$ to 3.7 doubles χ^2. Correspondingly $\log K_2$ and $\log K_3$ become 0.7 and 2.98, respectively (these are thus the upper limits as reported in Table II). Now, by decreasing $\log K_s$ by 2 orders of magnitude, i.e., setting it −0.1, the value of χ^2 remains almost unchanged (χ^2 = 1.44). This implies that a lower limit for $\log K_s$ cannot be given. The uncertainty on $\log K_2$ is also undetermined, because it changes from −0.06 to −3.1. On the other side, small relative variation is observed for $\log K_3$, which goes from 2.96 to 2.95 (its relative error on the lower limit is almost negligible). Therefore, for this parameter we can provide an error, i.e., the largest value between |2.98−2.96|=0.02 and |2.95−2.96|=0.01.

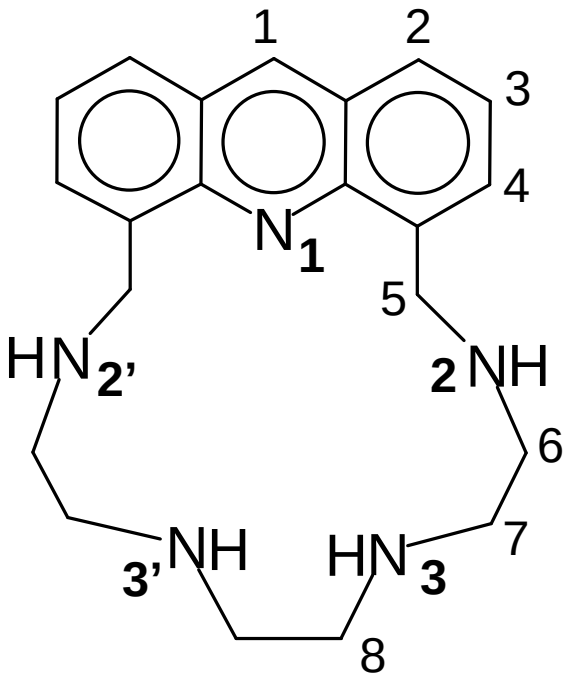

L

Figure 1

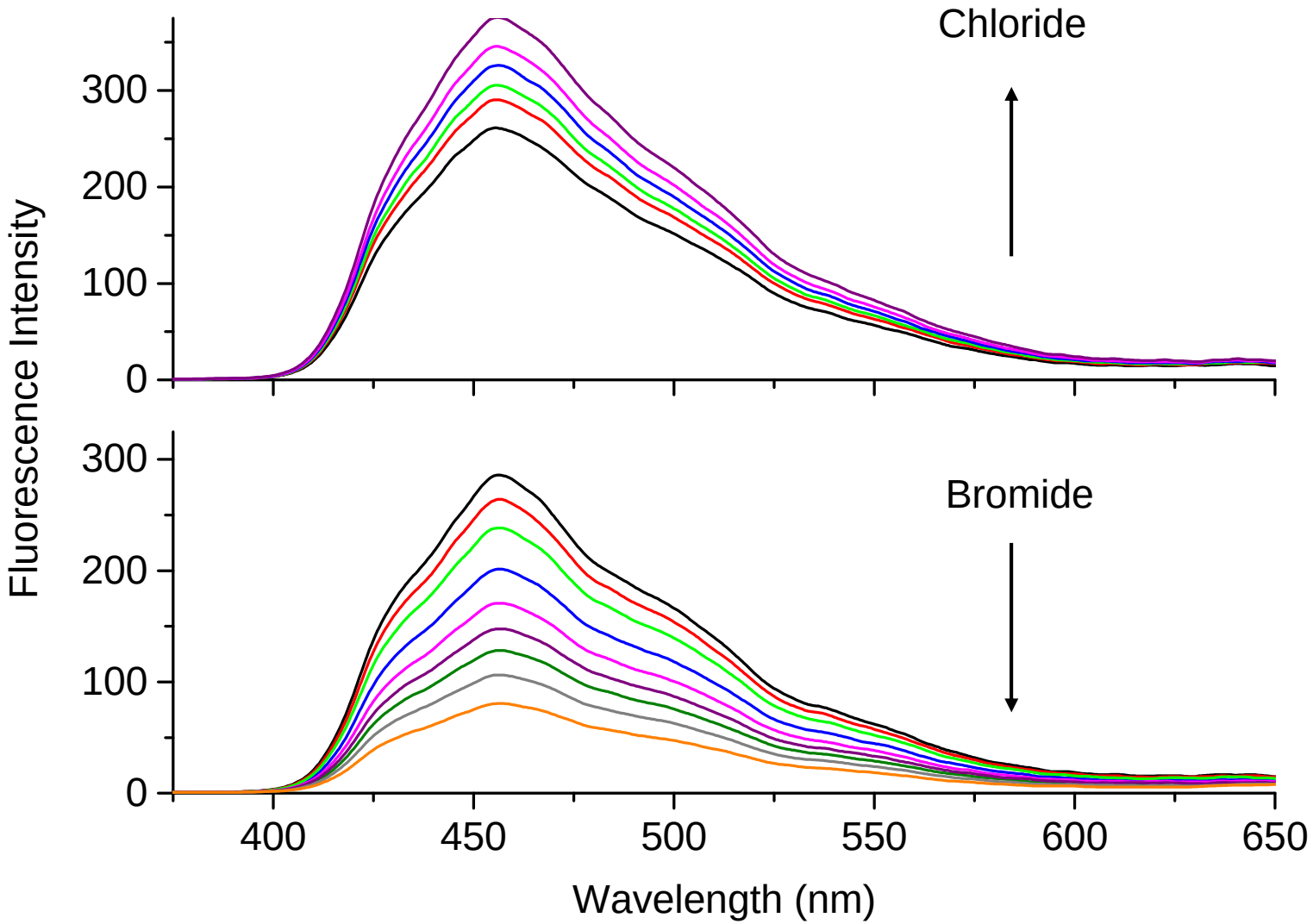

Figure 2

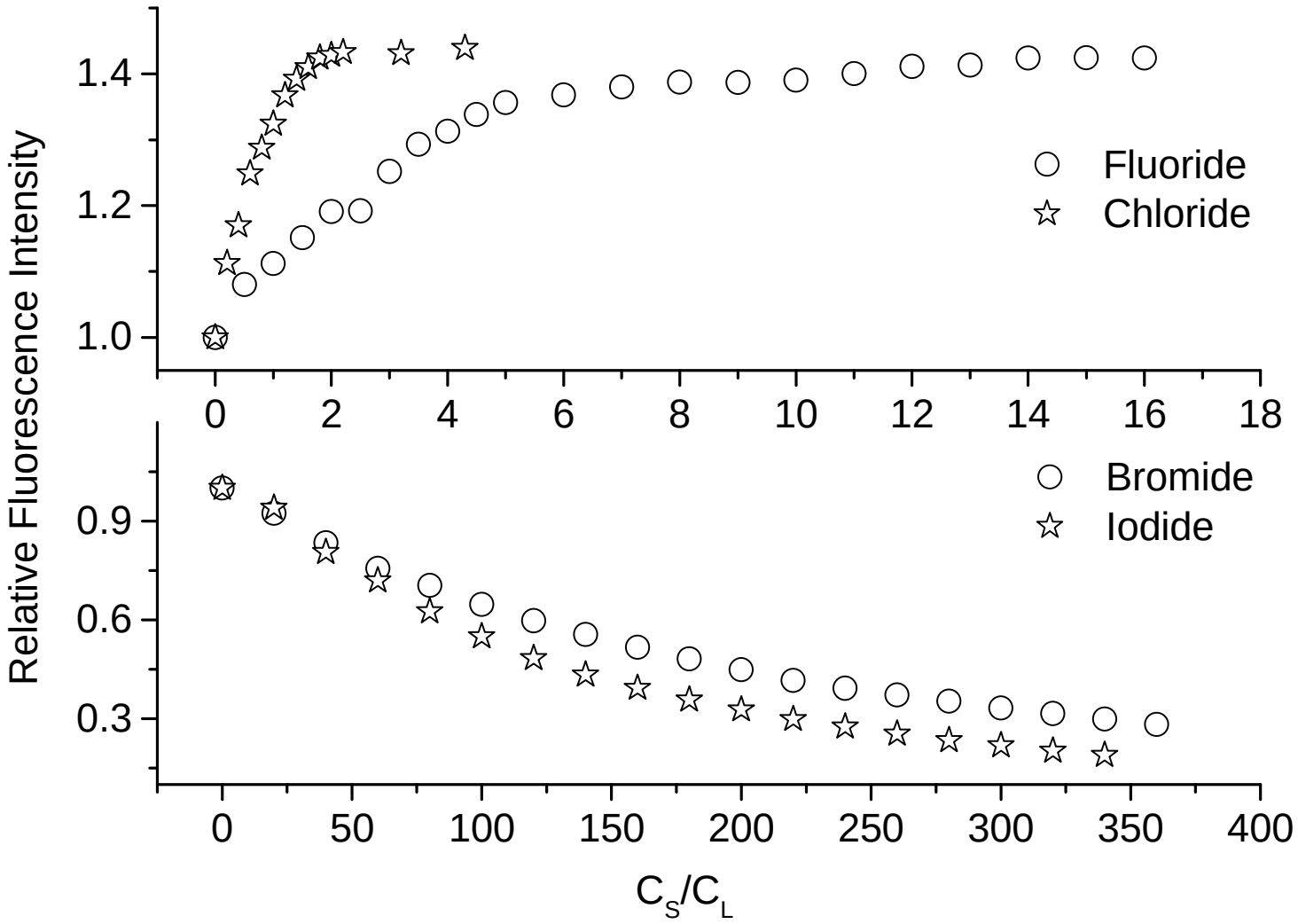

Figure 3

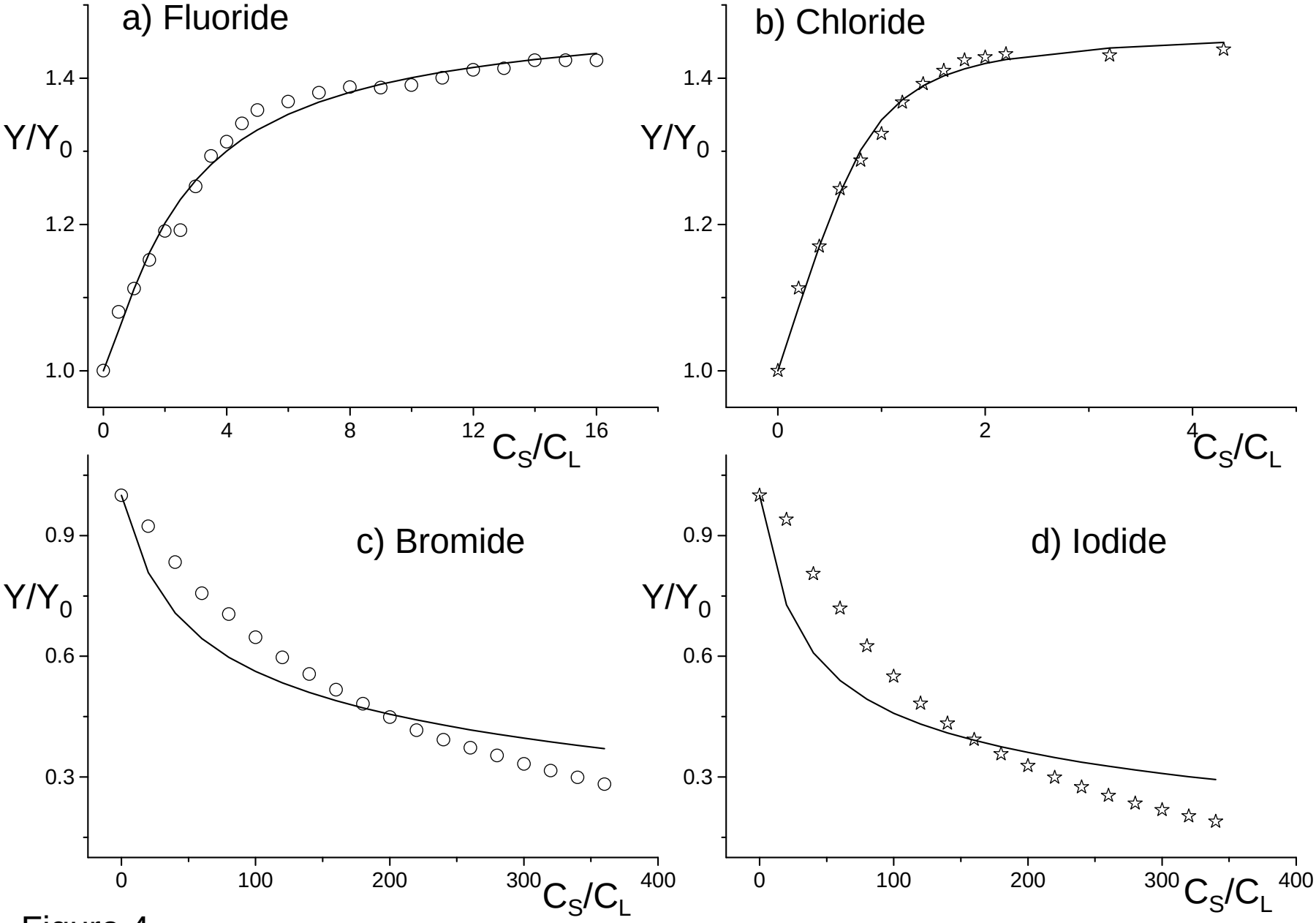

Figure 4

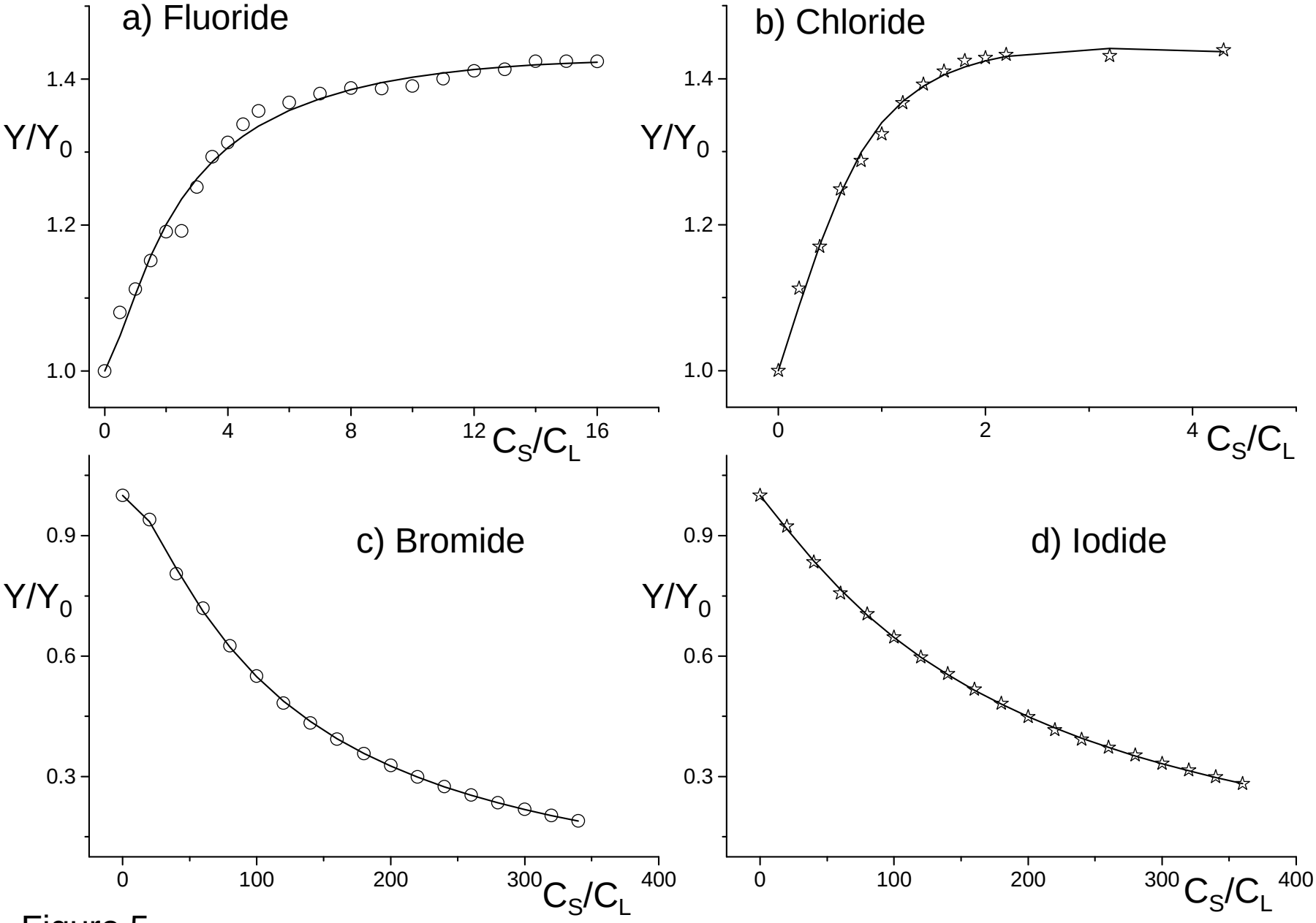

Figure 5

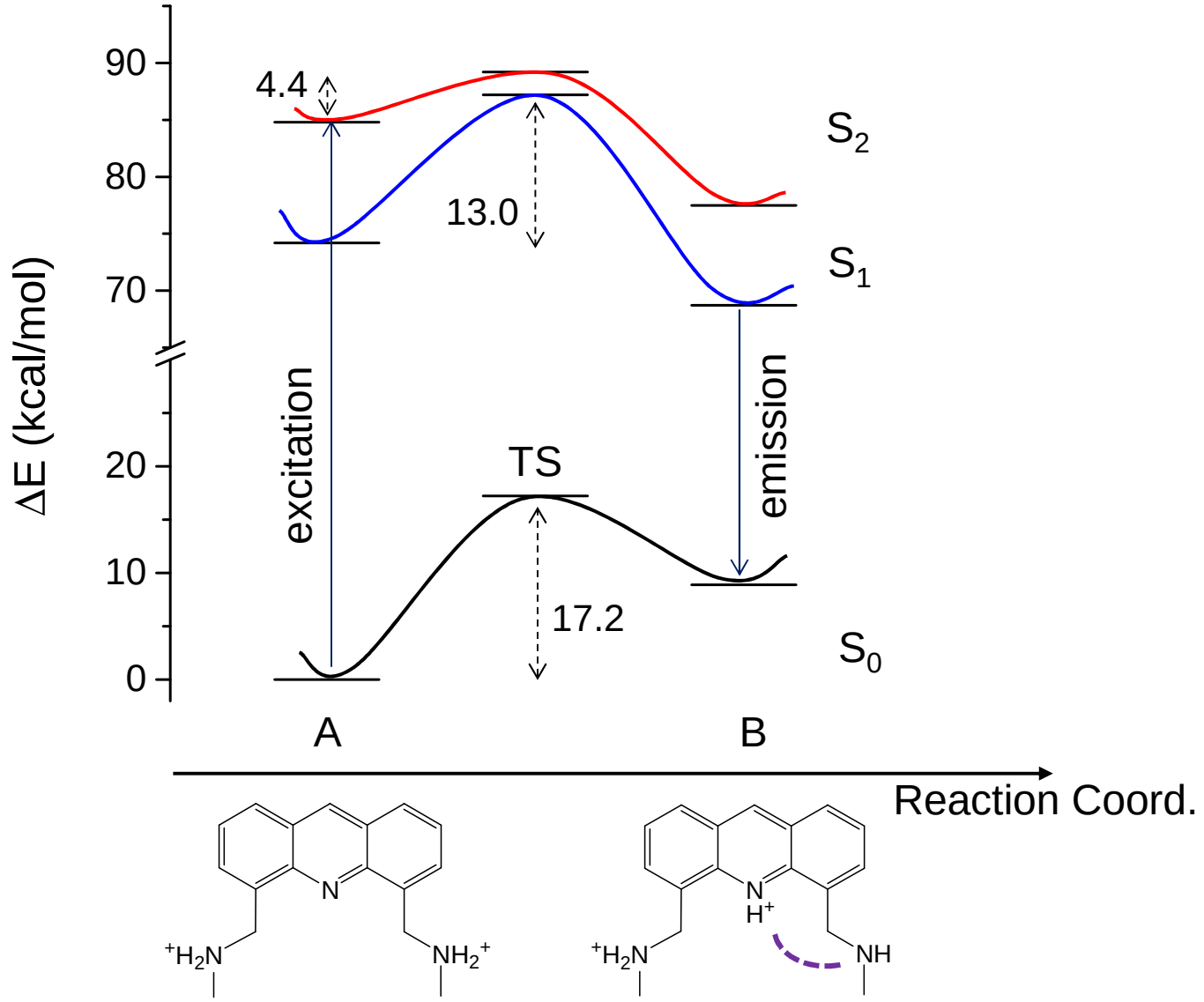

Figure 6

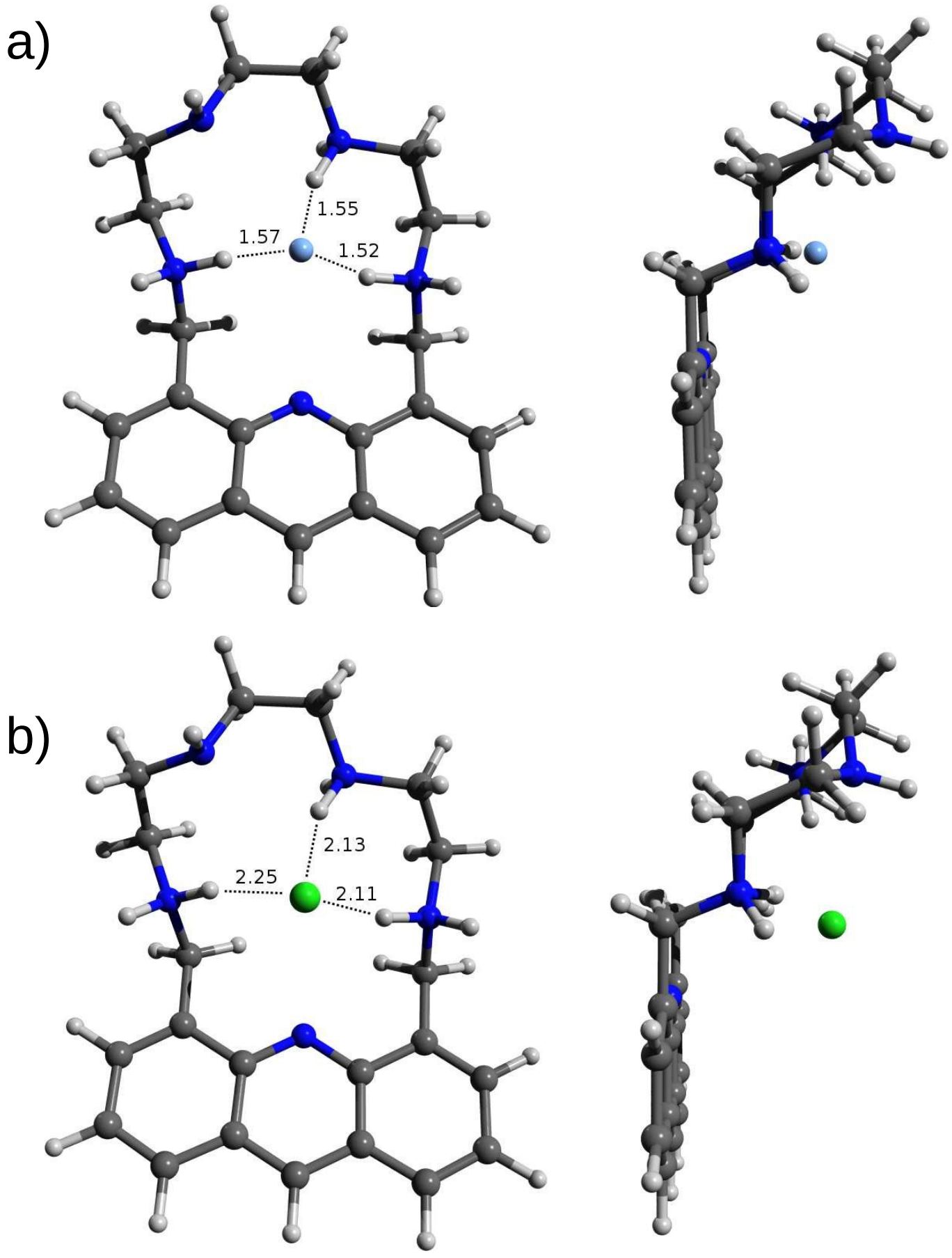

Figure 7